buildings

MDPI

Article

The Role of Xanthan Gum in Predicting Durability Properties of Self-Compacting Concrete (SCC) in Mix Designs

Alireza Masoumi [1], Reza Farokhzad [1,*] and Seyed Hooman Ghasemi [2]

[1] Department of Civil Engineering, Qazvin Branch, Islamic Azad University, Qazvin 82CM+Q6X, Iran; masoumi-ar@hotmail.com
[2] Department of Civil and Environmental Engineering, CREATES, Rowan University, 233 Rowan Hall, Glassboro, NJ 08028, USA; ghasemi@rowan.edu
* Correspondence: r.farokhzad@qiau.ac.ir

Abstract: This study comprehensively investigates the rheological properties of self-compacting concrete (SCC) and their impact on critical parameters, including the migration coefficient, penetration depth of chlorine ions, specific electrical resistance, and compressive strength. A total of 43 mix designs were meticulously examined to explore the relationships between these properties. Quantitative analysis employed a backpropagation neural network model with a single hidden layer to accurately predict the resistant and durable characteristics of self-compacting concrete. The optimal number of neurons in the hidden layer was determined using a fitting component selection method, implemented in MATLAB software(2021b). Additionally, qualitative analysis was conducted using sensitivity analysis and expert opinions to determine the priority of research additives. The main contributions of this paper lie in the exploration of SCC properties, the utilization of a neural network model for accurate prediction, and the prioritization of research additives through sensitivity analysis. The neural network model demonstrated exceptional performance in predicting test results, achieving a high accuracy rate using 14 neurons for predicting parameters such as chlorine penetration depth, compressive strength, migration coefficient, and specific electrical resistance. Sensitivity analysis revealed that xanthan gum emerged as the most influential additive, accounting for 43% of the observed effects, followed by nanomaterials at 35% and micro-silica at 21%.

Keywords: artificial neural networks; prediction model; rheological properties; self-compacting concrete; mix design

check for updates

Citation: Masoumi, A.; Farokhzad, R.; Ghasemi, S.H. The Role of Xanthan Gum in Predicting Durability Properties of Self-Compacting Concrete (SCC) in Mix Designs. *Buildings* **2023**, *13*, 2605. https://doi.org/10.3390/buildings13102605

Academic Editors: Xiaoyong Wang and Binsheng (Ben) Zhang

Received: 28 August 2023
Revised: 10 October 2023
Accepted: 11 October 2023
Published: 16 October 2023

Copyright: © 2023 by the authors. Licensee MDPI, Basel, Switzerland. This article is an open access article distributed under the terms and conditions of the Creative Commons Attribution (CC BY) license (https://creativecommons.org/licenses/by/4.0/).

1. Introduction

Self-compacting concrete (SCC), also known as fluent concrete, is a highly fluid concrete that can flow without the need for vibration [1]. It has gained significant popularity in the construction industry due to its superior characteristics compared to conventional concrete. The development of SCC originated in Japan in 1988 with the aim of creating a more durable concrete material [2]. Notable features of SCC include reduced labor costs, decreased construction time, and the elimination of vibration and noise during the construction process. SCC exhibits excellent flowability, even around densely reinforced areas, requiring lower pump pressure and resulting in a smooth surface finish. Furthermore, SCC prevents the formation of voids around reinforcements, leading to a growing global demand for this fluid concrete [1]. SCC offers numerous advantages over traditional concrete, including:

1. elimination of the requirement for vibration;
2. reduction in noise pollution
3. decreased construction time and labor cost;
4. improved interface between cement paste, aggregate, or reinforcement;
5. reduced permeability and enhanced concrete durability;

6. facilitation of constructability and ensuring optimal structural performance [3–5].

SCC is characterized by a high binder content and the inclusion of a superplasticizer, which enables the concrete to flow easily while maintaining the coarse aggregate in a viscous suspension. Typically, cement is used as the primary binder material in SCC, along with the addition of a filler material to optimize the rheological properties of the mixture [6]. Numerous studies have confirmed that the incorporation of chemical and mineral admixtures enhances the workability and strength development of concrete [7–10]. It improves productivity, flowability, self-leveling properties, and overall performance of the concrete. However, the production of self-compacting concrete (SCC) often relies on a trial-and-error approach. Therefore, it is crucial to determine the optimal proportions of various concrete mix components, including mineral and chemical admixtures. Hence, it is important for research to evaluate the effectiveness of using silica fume (SF) and superplasticizer (SP) in concrete mixtures [11]. In Figure 1, countries working in this area are shown and Iran is an active member among them.

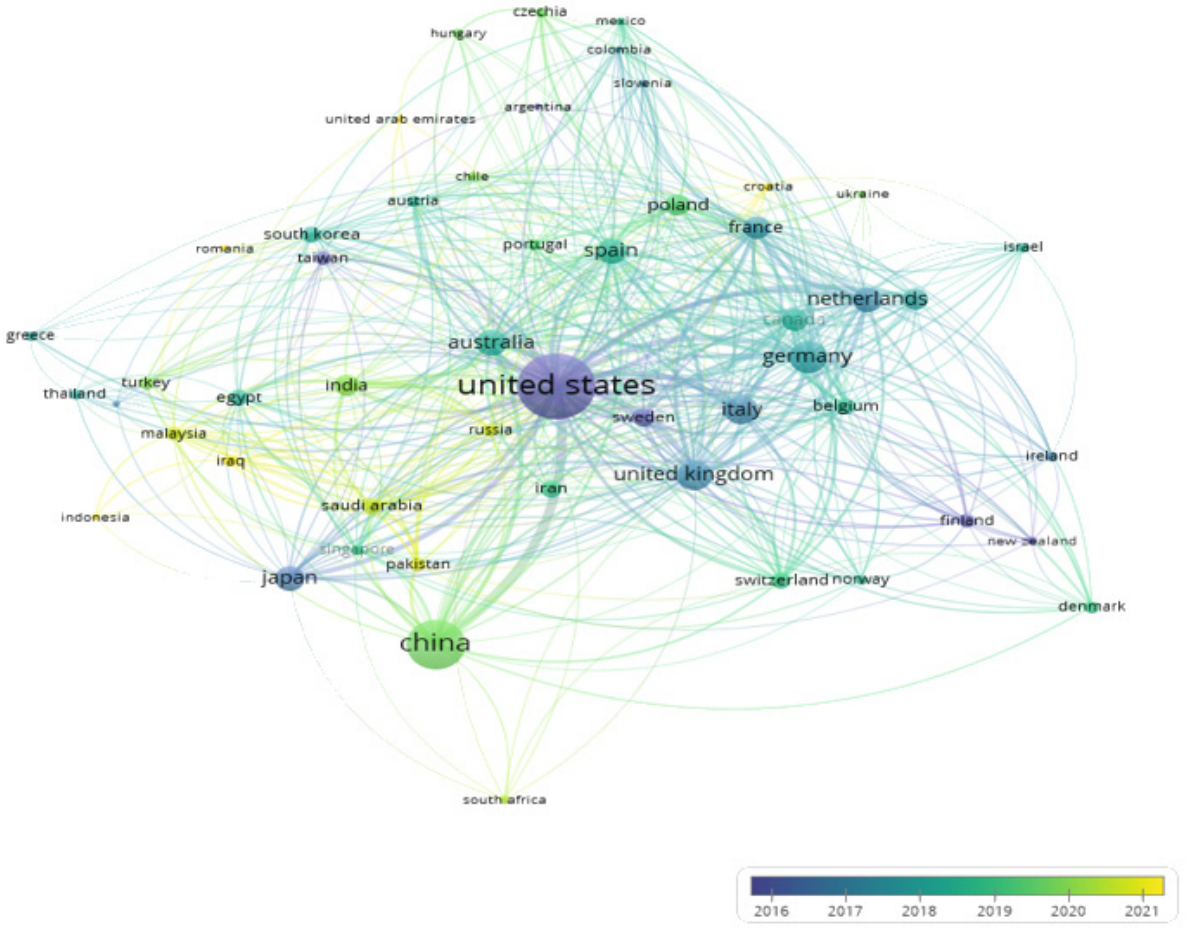

Figure 1. Research foci on mix design of SCC in different countries (VOS viewer software version 1.6.18).

To achieve high flowability in fresh self-compacting concrete (SCC) mixtures and to ensure desired durability in hardened SCC structures, specific types of chemical admixtures are often required. One crucial chemical admixture is superplasticizer (SP), which can effectively modify the rheological behavior of SCC by dispersing cement particles through electrostatic and/or steric repulsion mechanisms. While increasing the water-to-powder ratio can enhance the fluidity of concrete, it is important to avoid blindly increasing this ratio as it may adversely affect the mechanical properties of the concrete. The use of SP

ensures that SCC adequately fills the formwork and achieves complete compaction even at low water-to-powder ratios [12].

The properties of raw materials have a significant impact on the workability of SCC [13]. Recently, nanotechnology and nanomaterials have generated tremendous global interest due to their high performance in various fields. The main reason behind addition of nanomaterials into all types of concrete composites including SCC is to enhance the microstructural characteristics of the concrete composite. As a result, the commercial-scale use of nanotechnology in the concrete industry is still limited to a few available products in the market. Another challenge in utilizing nanomaterials is achieving their uniform distribution within the concrete matrix. Additionally, nanoparticles exhibit high water absorption due to their large specific surface area, which can impact concrete efficiency [10]. The addition of micro- and nano-silica (NS) resulted in improved properties of hardened concrete, leading to a better microstructure. This enhancement was particularly evident in the increased compressive and flexural strengths observed at 90 days due to the improved pozzolanic reactivity of silica particles [14,15]. In a study conducted by Dinesh [16], the fresh and hardened properties of self-compacting concrete (SCC) were investigated by partially replacing ordinary Portland cement with fly ash and silica fume. Different replacement percentages of 5%, 10%, 15%, 20%, and 25% of silica fume and fly ash were considered. Rao et al. [17] examined the variations in durability properties of self-compacting concrete (SCC) across different grades, ranging from low strength (M20 grade) to high strength (M70 grade). The investigation focused on durability aspects such as acid attack, corrosion, sorptivity, and thermal studies. Concrete specimens were exposed to 2% and 5% solutions of sulfuric acid and hydrochloric acid to assess their resistance to acid attacks.

The experimental investigations revealed that increasing the replacement percentages resulted in improved fresh and hardened properties of SCC. To assess the durability of self-compacting concrete (SCC) containing metakaolin (MS) as a replacement material for cement, tests were conducted using different percentages (5%, 10%, and 15%) of MS in M40 grade SCC. The performance of cementitious blends, such as ground granulated blast furnace slag and MS, was evaluated in terms of fresh and mechanical properties, with MS replacing 5% to 25% of the cement. The investigation of fresh concrete indicated that all the mixes produced met the minimum standard flow diameter requirements [18]. The combined effect of NS and MS was examined in the workability test, where SCC mixes containing both materials were cured in a sulfuric medium to assess durability. The combination of 5% MS and 1% NS exhibited 15.4% higher compressive strength than the control SCC mix at 28 days [19]. The performance of NS-blended cementitious systems was evaluated in terms of workability, hardened properties, and durability. Concrete containing 2% NS showed a significant improvement of 18.82% in splitting tensile strength compared to the control SCC mix at 28 days. Furthermore, results from the chloride penetration test indicated that 2% NS exhibited lower charge passed in coulombs, indicating better resistance to chloride penetration [20].

On the other hand, this study takes into consideration the utilization of xanthan gum as a natural material, driven by environmental considerations and the aim of enhancing concrete consistency. Xanthan gum, an anionic and complex exopolysaccharide derived from Xanthomonas campestris pv [21–23], is a key component in the production of SCC. Xanthan gum is a white to cream-colored powder that is soluble in warm or cold water but insoluble in most organic solvents. Compared to other organic solutions, xanthan gum solution exhibits high viscosity even at low concentrations, making it a desirable stabilizer/condenser. Xanthan gum solutions possess pseudo-plastic properties, which improve the quality of the final product, facilitate analysis, and ensure flowability specifications. These solutions are stable over a wide pH range, from acidic to basic conditions, and exhibit thermo-stability, setting them apart from other polysaccharide solutions. Xanthan gum is tasteless and is produced through the aerobic fermentation of pure carbohydrate Xanthomonas campestris [24–28].

Due to its unique rheological properties, xanthan gum finds applications in various industries, including food, toiletries, oil recovery, cosmetics, water-based paints, and as a stabilizer for emulsions and suspensions [28]. Xanthan gum is a polysaccharide with a long chain made of β-(4,1) D-glucose units and it possesses numerous trisaccharide side chains attached to it [29–31]. Xanthan gum exhibits unique rheological properties, making it a valuable ingredient in various industries. It finds applications in the food industry as a thickening agent, stabilizer, and emulsifier in products such as sauces, dressings, beverages, and baked goods. Xanthan gum is also utilized in toiletries, cosmetics, oil recovery processes, and as a stabilizer for emulsions and suspensions in water-based paints.

Farrokhzad and Jamali [32] conducted a study to examine the impact of xanthan gum additive on the mechanical properties and durability of concrete. Their findings indicated that the addition of xanthan gum led to a decrease in slump and segregation, as well as an increase in compressive strength due to the increased viscosity of the concrete. By enhancing the continuity between concrete materials and reducing voids and porosity, the capillarity coefficient of the concrete was reduced, and its electrical resistance increased. Microstructural investigations, including scanning electron microscope (SEM) tests, revealed that the use of xanthan gum resulted in decreased permeability and strengthened structural bonds within the concrete adhesive. Consequently, the samples containing xanthan gum exhibited lower porosity compared to the samples without it. Reinoso [33] conducted a study on the rheological properties of xanthan gum in saltwater solutions at high temperatures. The findings of their research demonstrated that xanthan gum enhances the density and viscosity of the fluid by increasing the salt concentration. Additionally, it expands the temperature range within which the solution displays viscoelastic behavior. Therefore, based on the findings of previous studies [32,33] which indicated that xanthan gum is a neutral thickening agent without harmful effects, and considering our objective of incorporating a thickening agent, we decided to include xanthan gum as a new additive in our experimental plans. The rheological behavior of self-compacting concrete will be more complicated when a variety of chemical additives are added at the same time.

Considering the significance of self-compacting concrete (SCC) and its expanding applications, there is a need for a comprehensive evaluation that encompasses multiple parameters to enhance its performance. Previous studies have primarily examined individual factors influencing SCC, but they have not considered the multi-parameter evaluation and simulation of SCC concrete. This study aims to address this gap by focusing on the utilization of new-generation chemical additives that enable the production of self-compacting concrete. Consequently, the objective of this research is to evaluate the combined effects of these factors and determine their priority in order to identify the optimal combination for SCC. This research focuses on the utilization of new-generation chemical additives that enable the production of self-compacting concrete. Xanthan gum, which can function as a thickening and stabilizing agent, is employed in this study as a viscosity-modifying additive with super-lubricant properties to create self-compacting concrete. The innovative aspect of this research lies in its novel approach to self-compacting concrete, which encompasses both the effective implementation and optimal properties of the structural and durability characteristics of concrete. Furthermore, it involves an analytical evaluation of the simultaneous use of nano- and micromaterials in self-compacting concrete, which warrants further investigation.

2. Experimental Program

Exprimnetal program of this study was designed to investigate rheological properties of SCC.

2.1. Materials

The materials utilized in this research include cement, limestone powder, aggregates, super-lubricating materials, and chemical additives such as micro-silica, nano-silica, and xanthan gum. The characteristics of these materials are presented below:

- Cement

The cement used was type 2 of Hegmatan Cement Factory in Hamedan, Iran.

- Limestone powder

The stone powder used in the study was obtained from limestone mines located in Hamadan, Iran.

- Aggregates

The aggregate used had a maximum size of 19 mm and was acquired from the Ekbatan concrete company in Hamedan, Iran, specifically from Seyyedan mine.

Super-plasticizer material

To achieve the desired efficiency in the mixing designs, polycarboxylate super-lubricants from Promix and Alborz brands were utilized.

- Water

The water used for sample preparation was sourced from Ekbatan Concrete Omran Factory, Iran, and it had a pH value of 5.9.

Chemical additives

- Nano-silica

The nano-silica used in the study was sourced from Isatis Yazd Company, Iran.

- Micro-silica

Purchased from the concrete clinic, this micro-silica is in the form of pozzolan powder. It has a light gray color, a specific weight of 2.5 g per cubic centimeter, and its particles are spherical and non-crystalline (amorphous).

- Xanthan gum

The xanthan gum used in this study was obtained from Elixir company, Iran. It should be noted that prior to use, the xanthan gum powder was mixed with a portion of mixing water and then added to the concrete mix.

The concrete used in this study was of type 2, and its physical and chemical properties are detailed in Table 1.

Table 1. Physical and chemical analyses of type-2 concrete.

Chemical Composition %	SiO_2%	Al_2O_3%	Fe_2O_3%	CaO%	MgO%	SO_3%	K_2O%	Na_2O%	LOI%	C_3A%
ISIRI-389 [34]	Min20	Max6	Max6	--	Max5	Max3	--	--	Max3	Max8
EN-197-1 (32.5R) [35]	--	--	--	--	--	Max3.5	--	--	Max5	--
Hegmatan Cement	21.27	4.95	4.03	62.95	1.55	2.26	0.65	0.49	2.11	6.3

Furthermore, Tables 2–4 present the physical and chemical composition of micro- and nano-silica.

Table 2. Chemical composition of micro-silica.

pH	CaO	S	MgO	Na_2O	C	Cl	Fe_2O_3	Al_2O_3	SiO_2
8	0.5–1	8	0.6–1.2	0.7–0.9	0.8–2	0.05–0.07	1.2–1.8	0.6–1.2	90–95

Table 3. Physical composition of micro-silica.

Mass Density kg/m^3	Specific Density	Structure	Particle Size	Color	Specific Surface m^2/g
310–350	2/2	amorphous	smaller than 1 μm	light gray	15–30

Table 4. Physical and chemical compositions of nano-silica.

Chemical Formula	SiO_2
Form	Ultrafine Amorphous Powder
Color	White
Odor	Odorless
Molecular Weight	60.08 g/mol
Specific Gravity (water = 1)	2.2
Bulk Density kg/m^3	90–110
pH Value	6.5–7.5 (5 Weight % Solid in Water)
Particle Size	80–100 nm

2.2. Rheological Measurements

The primary objective of this research is to determine a suitable mixing design for achieving self-compacting concrete with optimal strength. Additionally, the study aims to investigate various parameters that influence the efficiency of self-compacting concrete and to examine the rheological properties of self-compacting concrete using chemical additives in order to evaluate the desired parameters of the concrete. Self-compacting materials were prepared according to Table 5 and Figure 2. Each design underwent compressive strength tests; rheology tests including slump flow box L, J-ring [36], and V funnel [37]; rheometer tests; and durability tests including a permeability test, RCMT, and electrical resistance measurements. In this article, sensitivity analysis is used in a reliability method in combination with neural networks to identify the most effective substance. A flowchart is shown in Figure 2. In this article, sensitivity analysis is employed in conjunction with a reliability method and neural networks to determine the most influential substance. A flowchart outlining this approach is presented in Figure 2.

Table 5. The details of individual mix designs (kg/m^3).

Design Code	Cement	Xanthan Gum	Nano-Silica	Micro-Silica
SCC—7 days	400	0	0	0
SCC	400	0	0	0
Z (0.2)	399/2	0/8	0	0
Z (0.25)	399	1	0	0
SF (5)	380	0	0	20
SF (7)	372	0	0	28
SF (10)	360	0	0	40
Na (2)	392	0	8	0
Na (3)	388	0	12	0
Na (4)	384	0	16	0
Z(0.2) + SF(5)	379/2	0/8	0	20
Z(0.2) + SF(7)	371/2	0/8	0	28
Z(0.2) + SF(10)	359/2	0/8	0	40
Z(0.25) + SF(5)	379	1	0	20
Z(0.25) + SF(7)	371	1	0	28
Z(0.25) + SF(10)	359	1	0	40
Z(0.2) + SF(10) + Na(2)	351/2	0/8	8	40

Table 5. *Cont.*

Design Code	Cement	Xanthan Gum	Nano-Silica	Micro-Silica
Z(0.2) + SF(10) + Na(3)	347/2	0/8	12	40
Z(0.2) + SF(10) + Na(4)	343/2	0/8	16	40
Z(0.25) + SF(10) + Na(2)	351	1	8	40
Z(0.25) + SF(10) + Na(3)	347	1	12	40
Z(0.25) + SF(10) + Na(4)	343	1	16	40
Z(0.2) + Na 2	391/2	0/8	8	0
Z(0.2) + Na 3	387/2	0/8	12	0
Z(0.2) + Na 4	383/2	0/8	16	0
Z(0.25) + Na 2	391	1	8	0
Z(0.25) + Na 3	387	1	12	0
Z(0.25) + Na 4	383	1	16	0
Z(0.2) + SF(5) + Na(2)	371/2	0/8	8	20
Z(0.2) + SF(5) + Na(3)	367/2	0/8	12	20
Z(0.2) + SF(5) + Na(4)	363/2	0/8	16	20
Z(0.2) + SF(7) + Na(2)	363/2	0/8	8	28
Z(0.2) + SF(7) + Na(3)	359/2	0/8	12	28
Z(0.2) + SF(7) + Na(4)	355/2	0/8	16	28
Z(0.25) + SF(5) + Na(2)	371	1	8	20
Z(0.25) + SF(5) + Na(3)	367	1	12	20
Z(0.25) + SF(5) + Na(4)	363	1	16	20
Z(0.25) + SF(7) + Na(2)	363	1	8	28
Z(0.25) + SF(7) + Na(3)	359	1	12	28
Z(0.25) + SF(7) + Na(4)	355	1	16	28
Na(2) + SF(10)	352	0	8	40
SF(7) + Na(2)	364	0	8	28
SF(5) + Na(3)	368	0	12	20

2.3. Experimental Design

The design methods for concrete structures are generally similar globally, but each country incorporates specific calculations considering factors such as density, water requirements for workability, and strength based on locally available aggregates and cement. In this study, a water-to-cement ratio of 0.45 was utilized for the self-compacting concrete (SCC) mix design. The mix design followed the national standards of Iran, while the rheological properties were set according to the EFNARC guidelines [38]. It should be noted that in addition to utilizing the national mixing plan, we conducted extensive trial-and-error experiments to ensure the desired rheological properties. Based on these, various additives were introduced into the concrete mix to assess their performance. Xanthan gum was added at 0.2% and 0.25% of the concrete weight; micro-silica at 5%, 7%, and 10% of the concrete weight; and nano-silica at 2%, 3%, and 4% of the concrete weight. To evaluate the effects of these additives, single-additive designs, double-additive designs, and triple-additive designs were created and examined in each experiment. The design codes utilized were as follows: "SCC" represents self-compacting concrete, "Z" represents xanthan gum, "SF" represents micro-silica, and "Na" represents nano-silica. The numbers following each additive indicate the percentages by weight of the total concrete. For exam-

ple, "Z(0.2) + SF(5)" indicates SCC with 0.2% xanthan gum and 5% micro-silica by weight of the total concrete. Detailed information for each design can be found in Table 5.

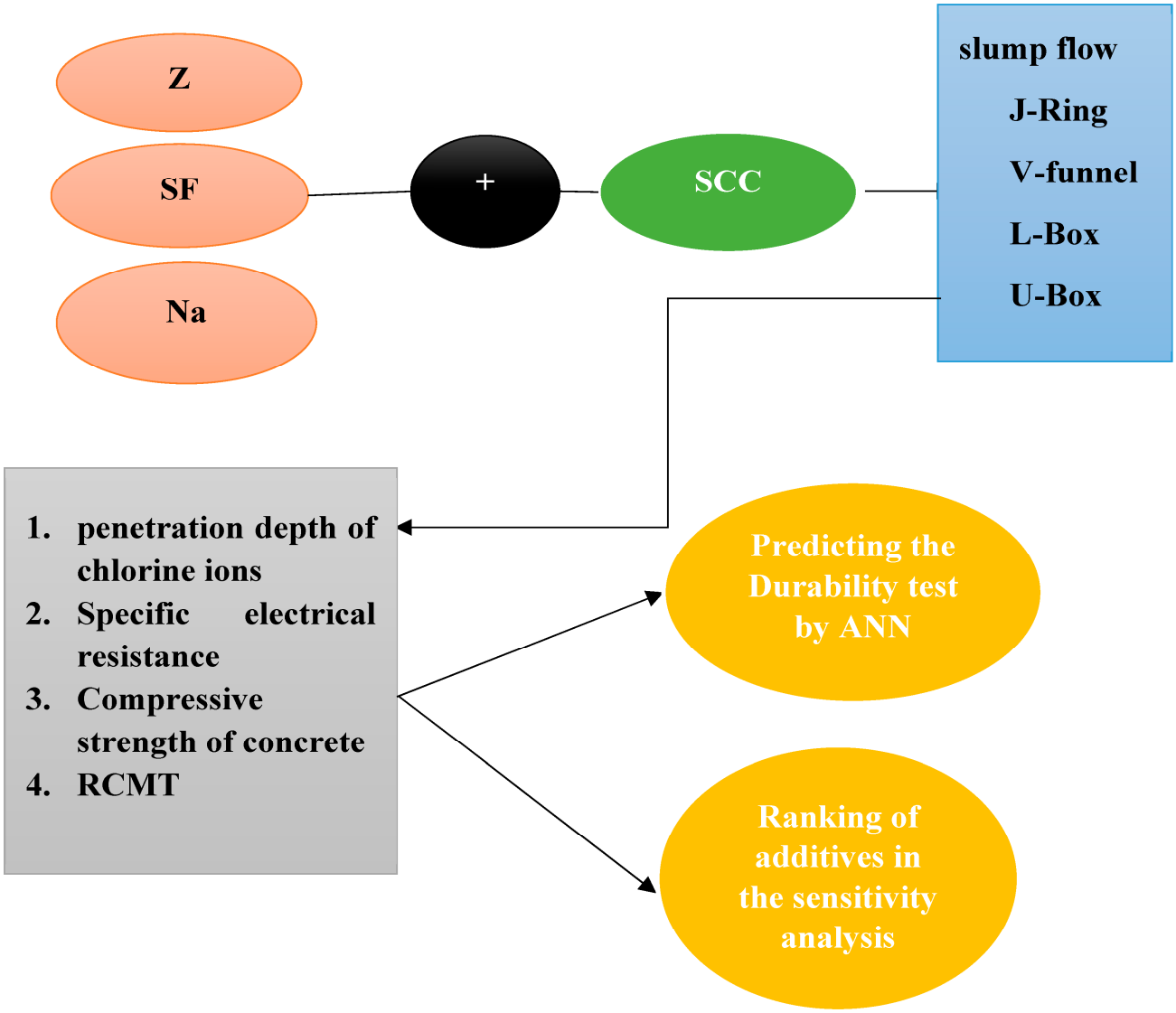

Figure 2. Flowchart of the study.

The experiments were conducted at two specific laboratories, namely Davam Bonyan and Sinab, both situated in the western region of Hamedan, Iran. The experimental procedure comprised two distinct components: mechanical tests and durability tests. In the initial phase, various parameters were evaluated at intervals of 7 and 28 days. These evaluations were conducted to examine the impact of concrete type, concrete quantity, and operational conditions on the outcomes (refer to Figure 3). The tests conducted in this study were performed in accordance with the following standards: compressive strength of concrete based on ISIRI [34] (Figure 4); specific electrical resistance based on the ASTM standard [39] (Figure 5); and RCMT and penetration depth of chlorine ions based on the AASHTO TP64–NTBUILD492 standards [40,41] (Figures 6 and 7).



Figure 3. The experimental design of the new SCC for reassurance of compliance with EFNARC guidelines.



Figure 4. Pressure resistivity test.



Figure 5. Electrical resistivity test.



Figure 6. Chloride ion penetration depth test.

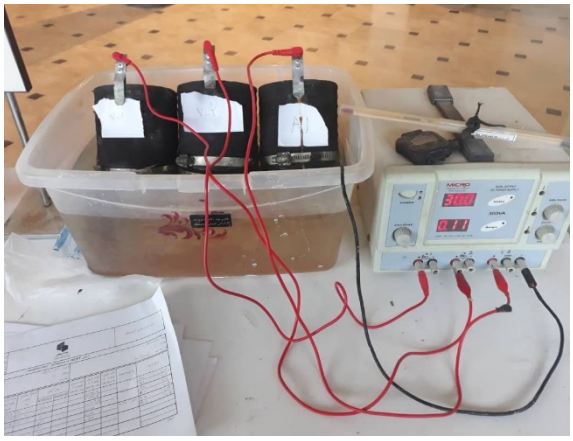

Figure 7. RCMT coefficient test.

3. The Artificial Neural Network

The artificial neural network (ANN) is a computational model inspired by the structure and functions of the human brain. Similar to the human brain, ANNs can learn from past data. The network learns by iteratively repeating the learning process. Once effectively trained on historical data, the ANN can accurately predict unknown inputs. An artificial neural network consists of multiple interconnected artificial neurons, organized in a specific network architecture. In the context of nucleus estimation, simple (nucleus) functions are located where any available case occurs, and their summation yields the estimator of the total probability density function [42]. Neurons act as the primary processing units, working in parallel. Each neuron conducts information processing by receiving inputs from other neurons and providing outputs for further processing. In this study, we employ the backpropagation (BP) neural network proposed in [43,44]. Following [45], a single hidden layer network is utilized. Based on our concrete mix proportioning database presented in Table 5, the neural network's input layer consists of four neurons, while the output layer comprises a single neuron representing parameters such as the migration coefficient, penetration depth of chlorine ions, specific electrical resistance, and compressive strength of concrete. The database is divided into two sets: the training set and the testing set. The structure of the BP-ANN employed in this study is illustrated in Figure 8.

In the network, $x_1, x_2,\ x_3,$ and x_4 are cement, micro-silica, nano-silica, and xanthan gum; due to the constant amount of water, we have not included this in the network. To ensure consistency, all input and output data in the artificial neural network (ANN) need to be normalized within the range of 0 to 1. This normalization process involves applying a linear transformation. Specifically, each variable is subtracted by its minimum value and divided by the range (maximum value minus minimum value) of that variable. By

using this linear transformation, all variables are scaled proportionally within the desired range [45].

$$\xi_i = \frac{x_i - x_{min}}{x_{max} - x_{min}} \quad (1)$$

$$\eta = \frac{y_i - y_{min}}{y_{max} - y_{min}} \quad (2)$$

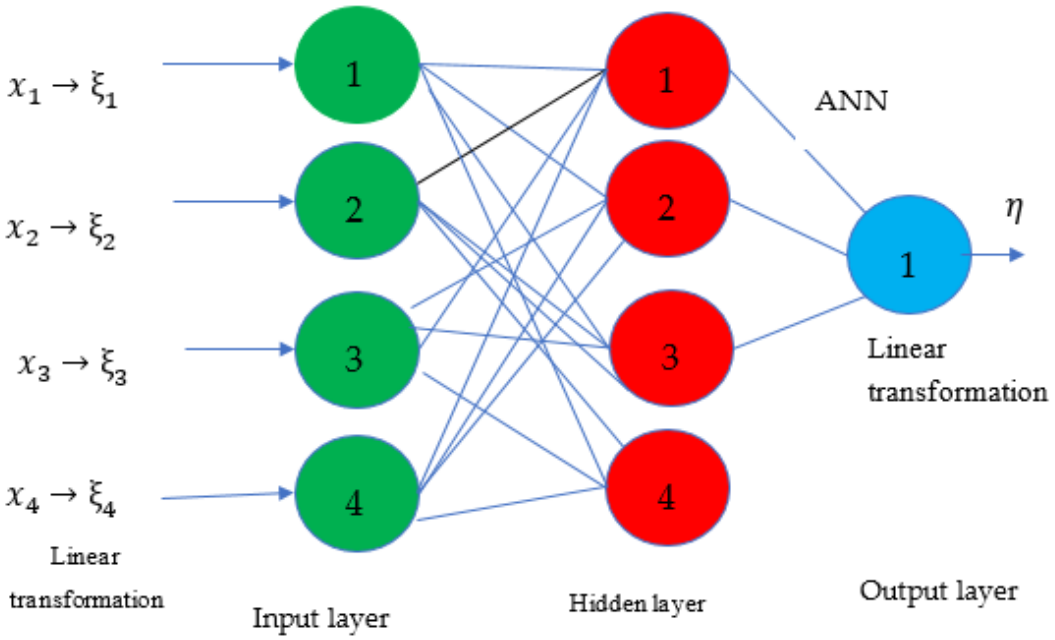

Figure 8. The input–output relation for predicting the durability test results of SCC and the structure of the ANN model.

4. Results of Experimental Design

The conducted tests encompassed two primary components: mechanical and durability assessments. In the mechanical aspect, the compressive strength after 28 days was evaluated to examine the impact of varying parameters such as concrete type, cement quantity, and processing conditions. The durability portion entailed tests on additional parameters, including specific electrical resistance, migration coefficient, and chlorine ion penetration depth, adhering to relevant regulations. The compressive strength values exhibited positive increments in double and triple mixed designs compared to the control design, resulting in a 35% enhancement. While a slight reduction was observed in the single design utilizing xanthan gum, the combination with micro- and nano-silica had an augmenting effect due to improved rheological properties, justifying its application.

Analyzing the penetration depth of chlorine ions in the control concrete (SCC), it was found that the age of the concrete influenced the depth. The concrete aged seven to twenty-eight days showed a 15% decrease in penetration depth. The migration coefficient of chlorine ions, an essential input for estimating the useful life and determining output parameters, was measured in various designs. The SCC design exhibited the highest migration coefficient, while the Z(0.2) + SF(7) + Na(2) design had the lowest. Interestingly, including xanthan gum alone positively reduced the migration coefficient. Notably, a significant decrease in migration coefficient values at 28 days compared to 7 days was observed, indicating a reduction of up to 15% as the samples aged. The concrete's ability to facilitate the transfer of ions within its microstructures, which infiltrate the concrete environment, relies heavily on the material's electrical resistance. In this study, the electrical resistance values reached an acceptable level, particularly in designs incorporating xanthan gum. The varied designs exhibited higher electrical resistance than the control

design, likely attributed to lower porosity and denser microstructure, with the triple design demonstrating the most significant increase. At 28 days, the specific electrical resistance experienced a 58% rise compared to 7 days. To summarize, the alterations in the examined parameters are depicted in Figure 9.

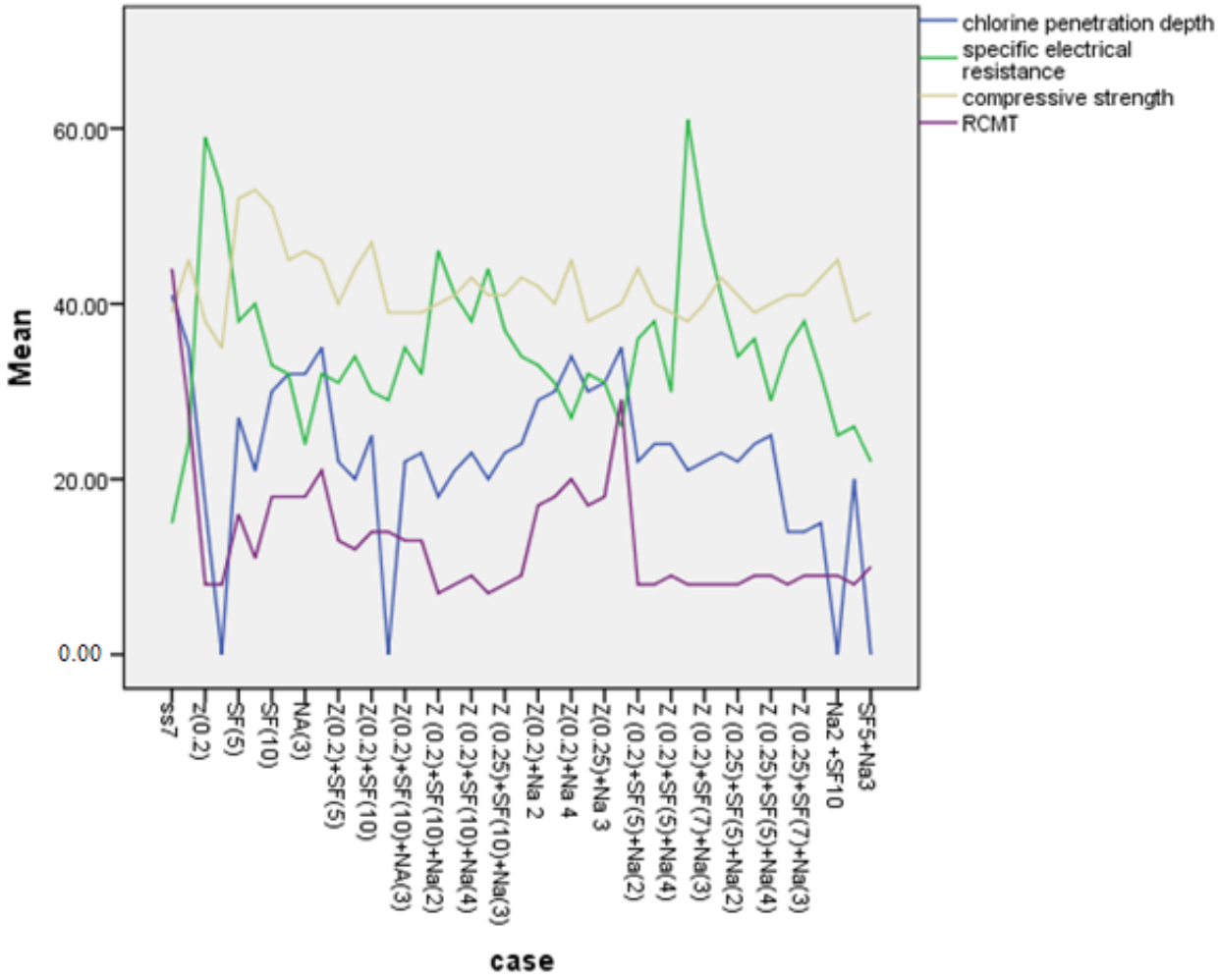

Figure 9. Changes in the parameters of the tests.

5. Neural Network Output

5.1. Prediction of the Chloride Ion Penetration Depth

Figure 10 illustrates the prediction of the chloride ion infiltration depth in concrete containing xanthan gum and micro- and nano-silica additives. These additives are being investigated to enhance the concrete's resistance against chloride ion penetration, which is crucial for ensuring the durability of structures in corrosive environments. A neural network with ten neurons was trained for this purpose. The figure also presents the error rates observed during the training, testing, and prediction phases. The neural network was trained using a dataset that included information about the concrete composition, proportions of additives, and chloride ion infiltration depth. The error rates provide an assessment of the model's accuracy at different stages. The error rate during the training phase measures the deviations between predicted and actual values in the training dataset. The test phase error rate evaluates the model's performance on an unseen dataset. Lastly, the prediction phase error rate indicates the model's accuracy when applied to new instances of concrete. Minimizing these error rates is crucial to enhance the reliability of the model for real-world applications in concrete technology and corrosion protection.

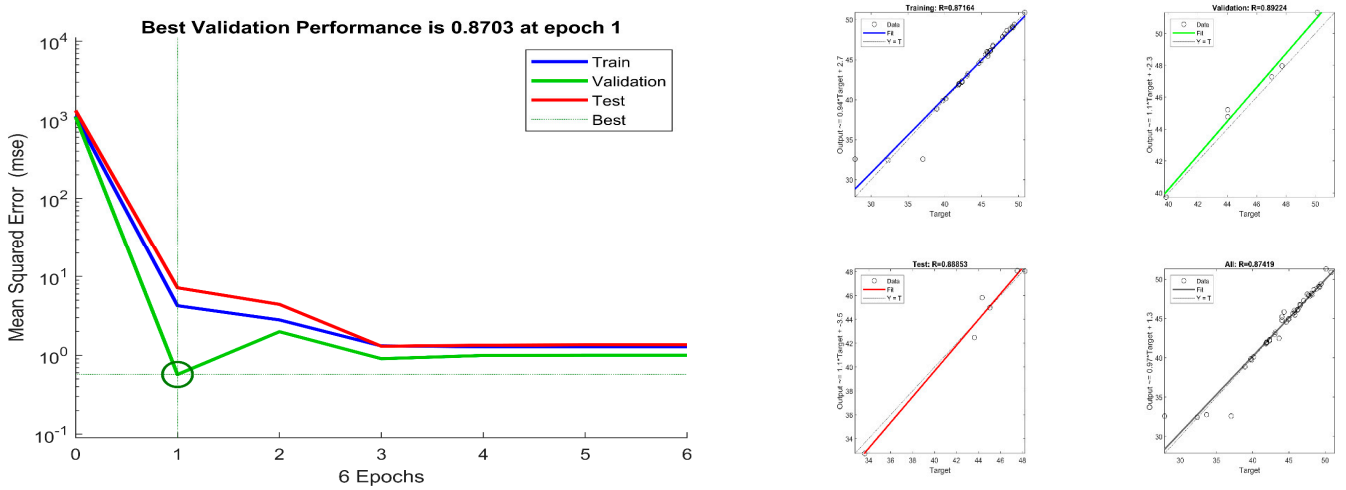

Figure 10. Prediction of the chloride ion infiltration depth in concrete containing xanthan gum, micro- and nano-silica, 10 neurons, and the error rates of the training, test, and prediction phases.

The results presented in Figure 11 offer a scientific perspective on predicting the depth of chloride ion infiltration in concrete when xanthan gum and micro- and nano-silica are incorporated, utilizing different neural network configurations. It is noteworthy that the correlation coefficient serves as an indicator of the strength and direction of the relationship between variables. In this case, a correlation coefficient of 87% is observed for the prediction of chloride ion penetration depth using ten neurons, suggesting a moderate positive correlation. On the other hand, utilizing 14 neurons leads to a significantly higher correlation coefficient of 91%, indicating a stronger positive relationship between the investigated additives and the infiltration behavior of chloride ions in the concrete.

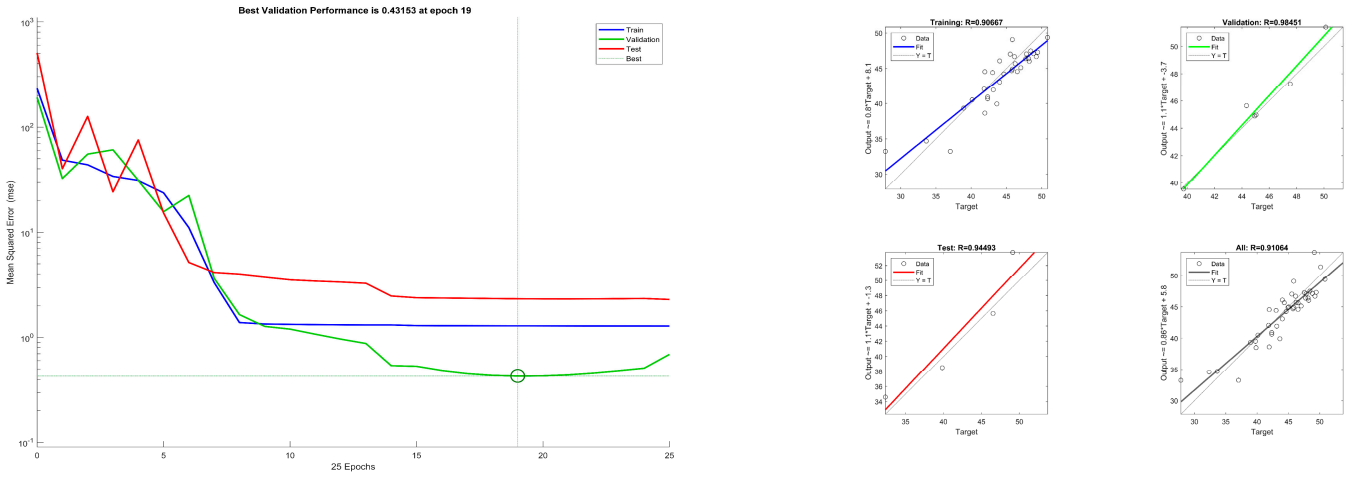

Figure 11. Prediction of the chloride ion infiltration depth in concrete containing xanthan gum, micro- and nano-silica, 14 neurons, and the error rates of the training, test, and prediction phases.

Additionally, the error rates in the training, test, and prediction phases, as evaluated using time series neural network models, provide insights into the accuracy of the predictions. A lower error rate implies a closer match between the predicted and actual values. In the case of 10 neurons, the error rate of 0.87 at epoch 1 indicates an average deviation of 87% from the actual values during the training, testing, and prediction phases. Similarly, when employing 14 neurons, the error rate decreases to 0.43 at epoch 19, indicating a slight improvement in prediction accuracy with an average deviation of approximately 43%.

These scientific observations highlight the potential of the neural network models in predicting the depth of chloride ion infiltration when incorporating xanthan gum and

micro- and nano-silica in concrete. However, it is essential to consider that these error rates indicate a significant margin of deviation from the actual values. Therefore, further optimization and refinement of the models may be required to enhance the accuracy and reliability of the predictions. It is also crucial to conduct further research and analysis to investigate the underlying mechanisms and variables contributing to the observed correlations and prediction errors.

5.2. Prediction of Electrical Resistivity

Figure 12 illustrates the electrical resistivity in concrete when incorporating xanthan gum and micro- and nano-silica additives. These additives are being investigated for their potential to enhance the electrical resistivity of concrete, which plays a crucial role in ensuring the durability of structures in corrosive environments. A neural network consisting of ten neurons was trained specifically for this purpose.

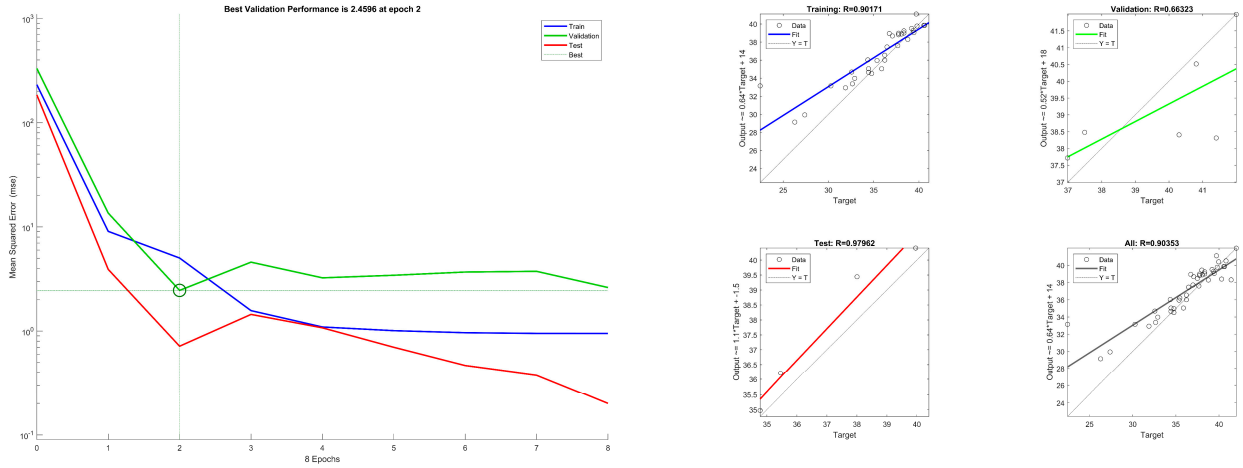

Figure 12. Prediction of the electrical resistivity in concrete containing xanthan gum, micro- and nano-silica, 10 neurons, and the error rates of the training, test, and prediction phases.

The results presented in Figure 13 provide a scientific perspective on the prediction of electrical resistivity in concrete when incorporating xanthan gum and micro- and nano-silica additives, using different neural network configurations. In this case, a correlation coefficient of 90% is observed for the prediction of electrical resistivity using 10 neurons, suggesting positive high correlation. However, when utilizing 14 neurons, the correlation coefficient increases to 97%, indicating a moderate stronger positive relationship between the investigated additives and the electrical resistivity in the concrete.

Furthermore, in terms of error rates for the neural network with 10 neurons, an error rate of 2.45 is observed at epoch 2. On the other hand, when employing 14 neurons, the error rate decreases to 0.48 at epoch 11, indicating a slight improvement in prediction accuracy. However, it is important to note that these error rates indicate a significant margin of deviation from the actual values. Therefore, further optimization and refinement of the models may be necessary to enhance the accuracy and reliability of the predictions. Additionally, conducting further research and analysis is crucial to investigate the underlying mechanisms and variables contributing to the observed correlations and prediction errors.

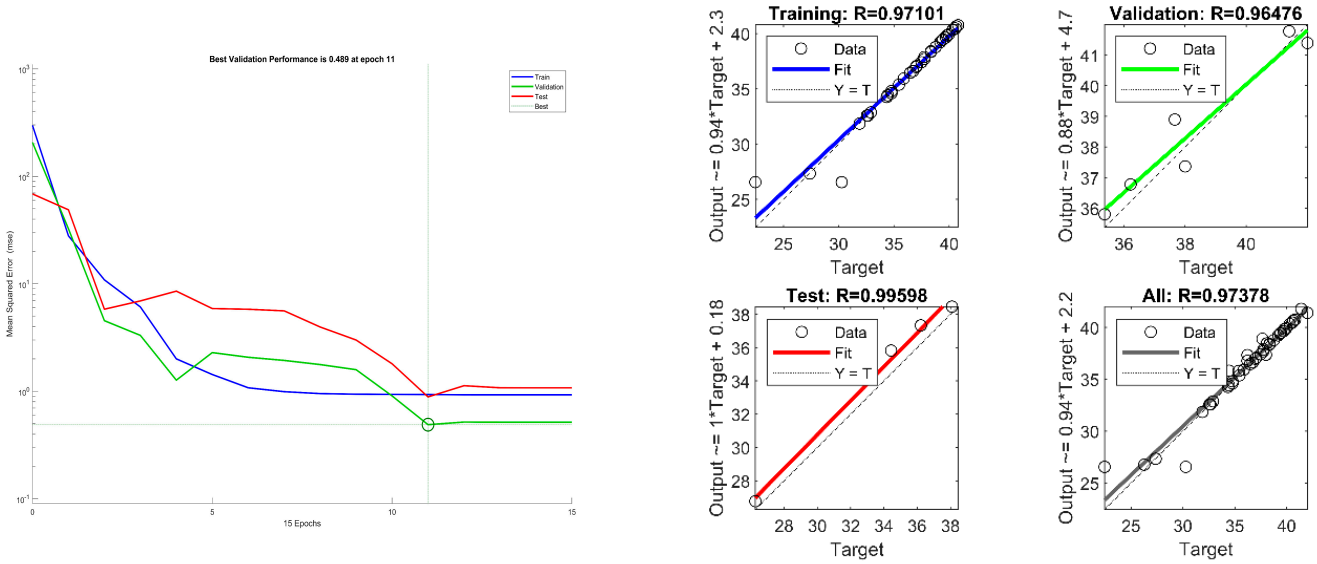

Figure 13. Prediction of the electrical resistivity in concrete containing xanthan gum, micro- and nano-silica, 14 neurons, and the error rates of the training, test, and prediction phases.

5.3. Prediction of Pressure Resistivity

Figure 14 illustrates the prediction of the pressure resistivity in concrete containing xanthan gum and micro- and nano-silica additives. These additives are being investigated to enhance the concrete's ability to withstand pressure, which is crucial for ensuring the durability of structures in corrosive environments. A neural network with ten neurons was trained for this purpose. The figure also presents the error rates observed during the training, testing, and prediction phases.

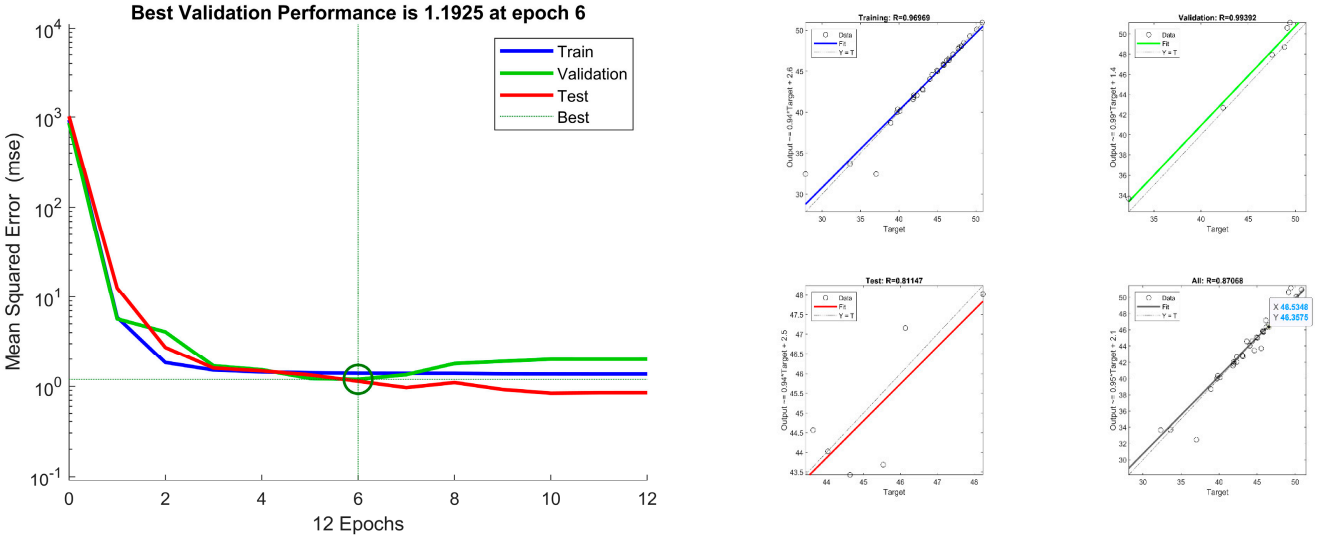

Figure 14. Prediction of the pressure resistivity in concrete containing xanthan gum, micro- and nano-silica, 10 neurons, and the error rates of the of training, test, and prediction phases.

The results presented in Figure 15 provide a scientific perspective on predicting pressure resistivity in concrete when xanthan gum and micro- and nano-silica additives are incorporated using different neural network configurations. The correlation coefficients obtained indicate the strength of the relationship between the investigated additives and the pressure resistivity in the concrete. With ten neurons, a correlation coefficient of 87% is observed, suggesting a moderate positive correlation. However, using 14 neurons leads to a

significantly higher correlation coefficient of 96%, indicating a stronger positive relationship between the additives and the pressure resistivity.

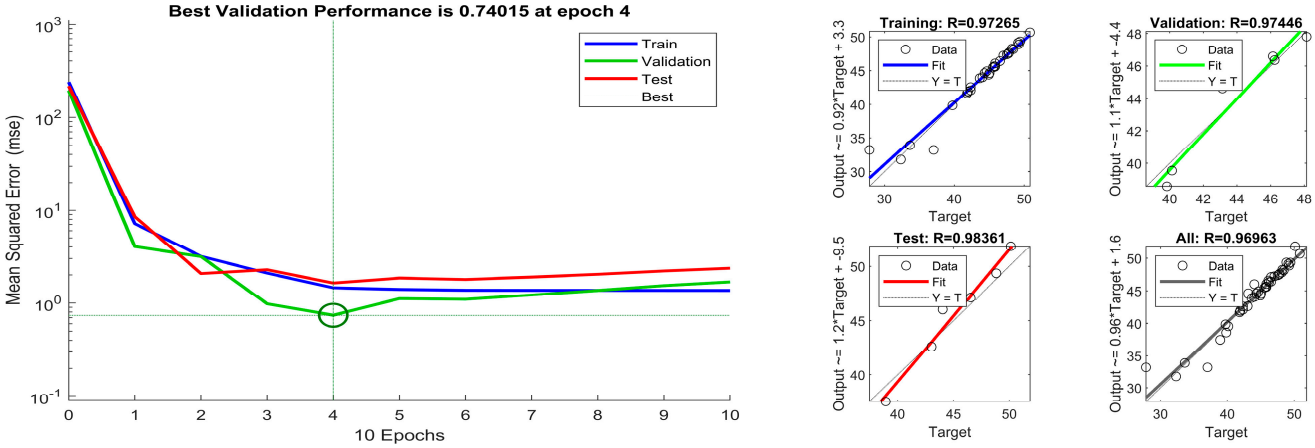

Figure 15. Prediction of the pressure resistivity in concrete containing xanthan gum, micro- and nano-silica, 14 neurons, and the error rates of the training, test, and prediction phases.

Moreover, the error rates in the training, test, and prediction phases, evaluated using time series neural network models, provide insights into the accuracy of the predictions. For the model with 10 neurons, the error rate starts at 1.19 at epoch 6. In contrast, the model with 14 neurons shows a decreased error rate of 0.74 at epoch 4, indicating a substantial improvement in prediction accuracy with an average deviation of approximately 74%. These scientific observations highlight the potential of neural network models in predicting pressure resistivity when xanthan gum and micro- and nano-silica are incorporated into concrete.

5.4. Prediction of RCMT Coefficient

Figure 16 depicts the RCMT coefficient in concrete with the inclusion of xanthan gum and micro- and nano-silica additives. These additives are being investigated to enhance the concrete's RCMT coefficient, which plays a critical role in the durability of structures exposed to corrosive environments. A neural network with 10 neurons was trained specifically for this purpose. The figure also provides information on the error rates observed during the training, testing, and prediction phases.

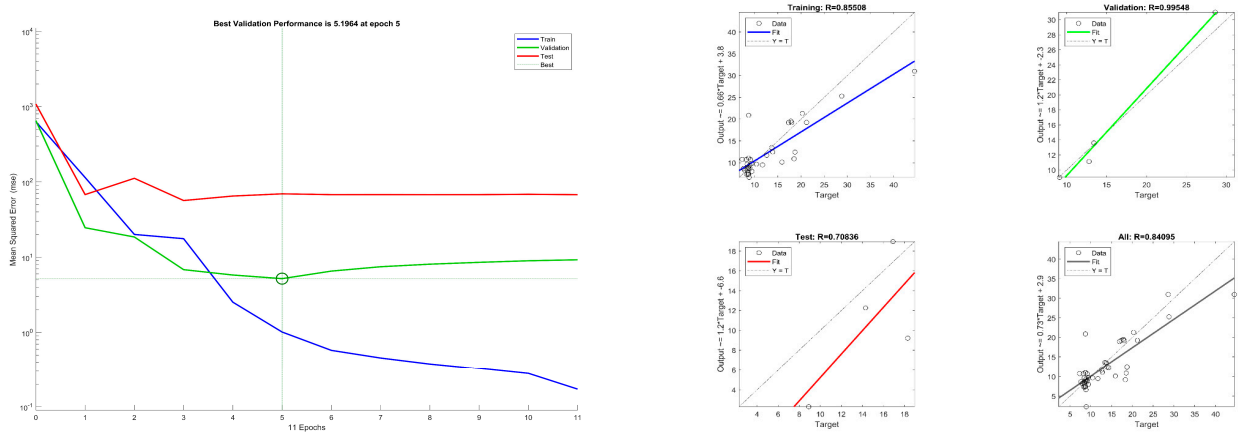

Figure 16. Prediction of the RCMT coefficient in concrete containing xanthan gum, micro- and nano-silica, 10 neurons, and the error rates of the training, test, and prediction phases.

The results presented in Figure 17 offer a scientific perspective on predicting pressure resistivity in concrete when incorporating xanthan gum and micro- and nano-silica with different neural network configurations. With 10 neurons, a correlation coefficient of 84% is observed for the prediction of the RCMT coefficient, indicating a moderate positive correlation. Conversely, utilizing 14 neurons yields a significantly higher correlation coefficient of 96%, indicating a stronger positive relationship between the investigated additives and the RCMT coefficient in the concrete.

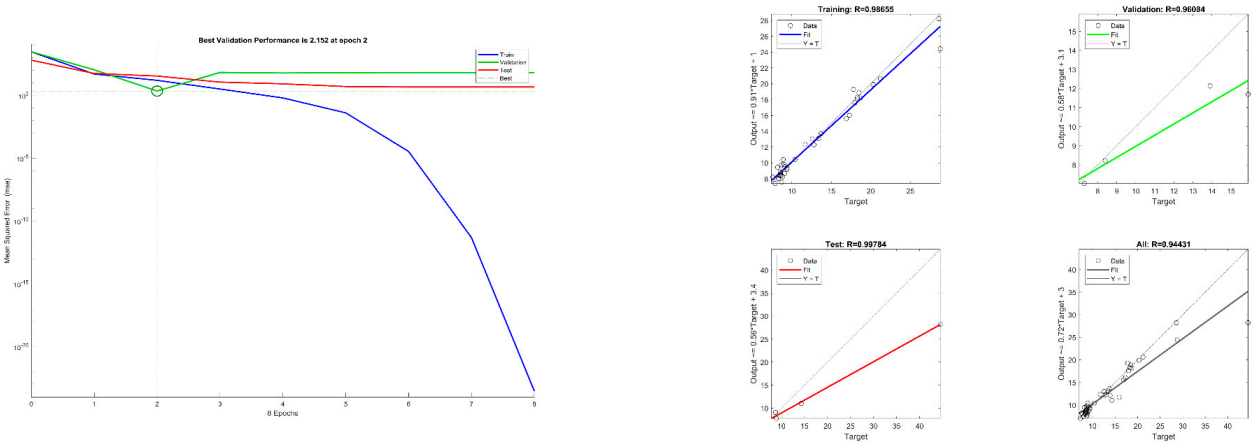

Figure 17. Prediction of the RCMT coefficient in concrete containing xanthan gum, micro- and nano-silica, 14 neurons, and the error rates of the training, test, and prediction phase.

Additionally, in the case of 10 neurons, an error rate of 5.19 is observed at epoch 5. Conversely, when employing 14 neurons, the error rate decreases to 2.15 at epoch 2, signifying a substantial improvement in prediction accuracy with an average deviation of approximately 78%.

These scientific observations underscore the potential of neural network models in predicting the RCMT coefficient when incorporating xanthan gum and micro- and nano-silica additives into concrete.

6. Sensitivity Analysis Results

A sensitivity analysis, specifically focusing on priority determination of additives, has been conducted in this study. The proposed model utilizes a three-level decomposition process to assess the durability parameters. The objective criteria used for evaluating durability include compressive strength (P), specific strength (S), penetration depth (C), and migration coefficient (R). These criteria are further evaluated using single, double, and triple concrete mix designs, with composite factors serving as sub-criteria. The research additives under evaluation are xanthan gum, nano-silica, and micro-silica. To facilitate the analysis, expert opinions have been incorporated to construct a comparison matrix.

The basic design of the model involves a comprehensive assessment of various durability parameters and additives, aiming to determine their relative performance and prioritize their usage in concrete applications (as depicted in Figure 18). This sensitivity analysis approach enables a detailed evaluation of the effectiveness of different additives in improving concrete properties and durability.

Figure 19 presents the achieved priority for the studied additives.

According to the analysis, xanthan gum is determined to be the most effective material with a priority rating of 43%. It is followed by nano-silica with a priority rating of 35%, and finally, micro-silica with a priority rating of 21%. Table 6 displays the ratings for the ideal, normal, and raw criteria. These findings provide valuable insights into the relative effectiveness and prioritization of the studied additives. They indicate that xanthan gum demonstrates the highest potential for enhancing concrete properties, followed by nano-silica and micro-silica.

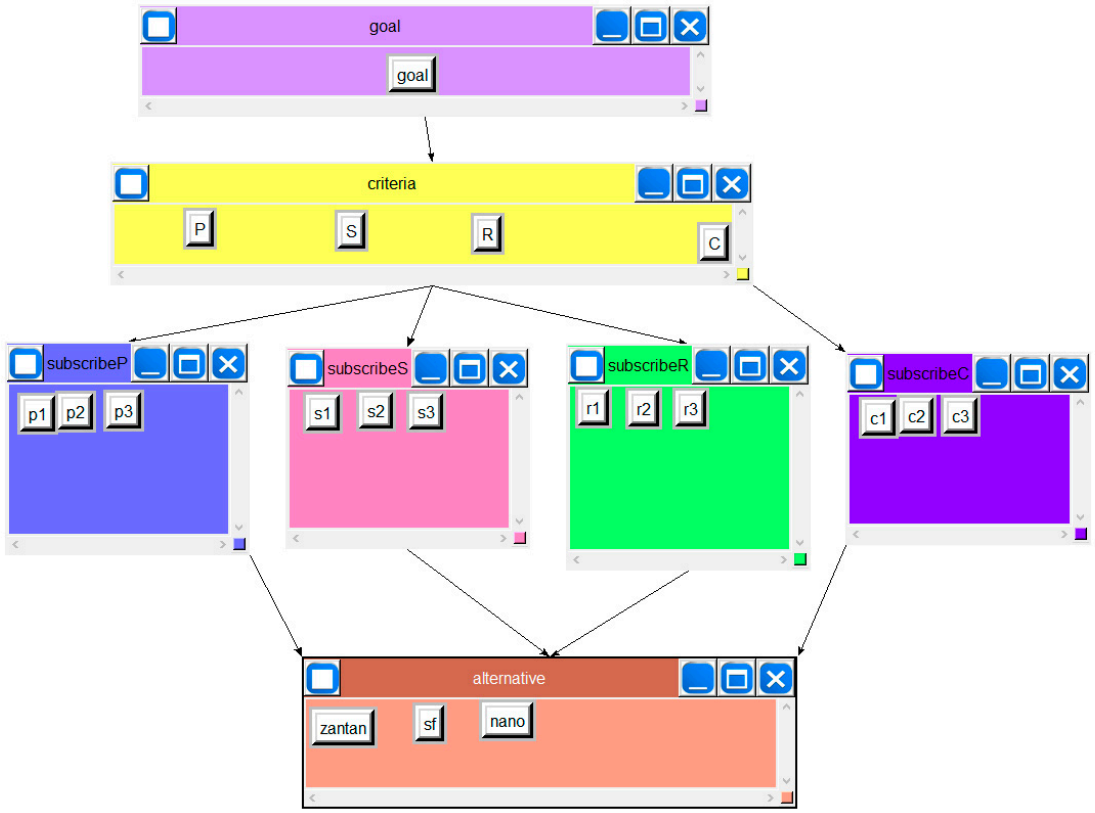

Figure 18. The architecture of sensitivity analysis in Super Decision.

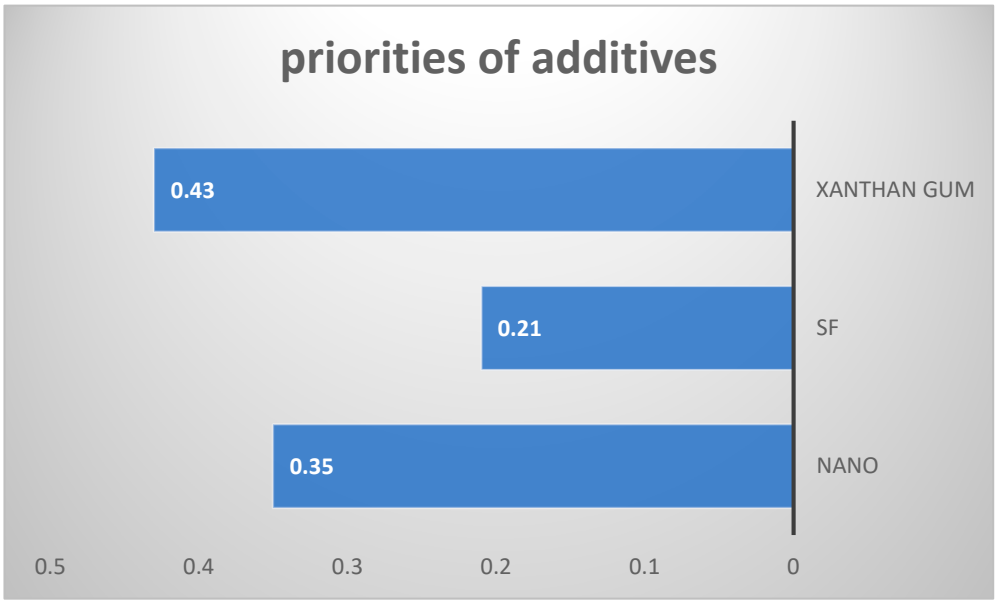

Figure 19. The ranking of the additives in the sensitivity analysis.

Table 6. Ideal, normal, and raw ratings of study additives.

Name	Ideal	Normal	Raw
Nano	0.82	0.35	0.36
SF	0.49	0.21	0.21
Xanthan gum	1.00	0.43	0.43

7. Discussion

Based on the conducted investigations, it can be concluded that the successful utilization of xanthan gum, micro-silica, and nano-silica particles as substitutes for cement in self-compacting concrete (SCC) has been achieved. However, it is important to note that increasing the percentage of micro- and nano-silica can decrease the flowability and permeability of fresh concrete. To maintain the desired efficiency, higher doses of super-lubricant in combination with xanthan gum, micro-silica, and nano-silica were employed. Notably, the composite mixtures met all the performance evaluation tests set by the European Federation of National Associations of Specialist Contractors (EFNARC). Nano-silica, with its small particle size and large specific surface area, plays a significant role in the concrete mixing process. The abundance of unsaturated bonds in nano-silica allows it to absorb a greater amount of water molecules, thereby reducing the slump of the concrete. This improved hydration of the concrete leads to the production of a higher quantity of C-S-H gel, which fills the pores of the concrete matrix, ultimately enhancing its overall performance. Additionally, nano-silica plays a crucial role in filling voids within the concrete. It effectively reduces the volume of pores, resulting in a more compact concrete structure. As a result, concrete modified with nano-silica exhibits excellent durability. Nano-silica also possesses higher pozzolanic activity. During the early stages, the enhancement of initial strength in nano-silica concrete is more pronounced due to a sufficient pozzolanic reaction. However, as the curing time progresses, the nano-silica particles gradually decrease in size, leading to a weaker pozzolanic response. Consequently, the impact of nano-silica on concrete strength improvement diminishes in the later stages. Micro-silica, on the other hand, reacts with lime during cement hydration to form calcium silicate hydrates (C-S-H). This process binds various components together and facilitates the creation of a dense and compact cement matrix. The pozzolanic properties of micro-silica enable it to exhibit high reactivity with the calcium hydroxide ($Ca(OH)_2$) generated during cement hydration. This high reactivity contributes to achieving significantly higher compressive strength, thereby extending the lifespan of the concrete. Xanthan gum demonstrates a distinctive retarding effect. During the initial stage of cement hydration, xanthan gum is adsorbed onto the surface of cement particles and forms complexes with calcium ions (Ca^{2+}). This process accelerates the dissolution of tricalcium aluminate (C_3A) to some extent while simultaneously slowing down the hydration reaction and preventing the premature formation of gel-like materials. Concrete samples containing xanthan gum exhibit lower porosity compared to the samples without xanthan gum. Moreover, the hydration products within the concrete structure containing xanthan gum exhibit a denser and more compact arrangement, thereby enhancing the consistency and durability of the samples. The experimental investigation conducted in this study has provided valuable insights into the behavior of concrete mix designs with different additives. Here are the key findings below.

1. Penetration Depth. The self-compacting concrete (SCC) mix had the highest penetration depth at 28 days, while the SF10 + Na2 design had the lowest. The inclusion of 2% nano-silica and 10% micro-silica resulted in a significant reduction in penetration depth. Xanthan gum used as a standalone additive also led to a substantial reduction of approximately 50% in penetration depth, indicating its positive impact on durability. Combining xanthan gum and micro-silica at varying percentages showed notable reductions in penetration depth. Adding 5%, 7%, and 10% micro-silica resulted in depth reductions of 37%, 41%, and 29%, respectively, compared to the control concrete. Similarly, incorporating xanthan gum with nano-silica at percentages of 2%, 3%, and 4% yielded depth reductions of 16%, 14%, and 2%, respectively. These findings suggest that these additive combinations can enhance the resistance of concrete to chloride ion penetration.
2. Compressive Strength. The double and triple mix designs exhibited an improved compressive strength compared to the control design, with an increase of up to 35%. This indicates that the selected additives positively influenced the mechanical properties of the concrete, potentially contributing to its overall strength and durability.

3. Migration Coefficient. All additives demonstrated a decreasing effect on the migration coefficient, which implies the improved resistance to chloride ion migration. In dual additive designs, incorporating xanthan gum with micro-silica at different percentages resulted in substantial reductions in the migration coefficient. The combination of xanthan gum and nano-silica also yielded significant reductions. Among the triple additive designs, the Z(0.2) + SF(7) + Na(2) configuration showed the most significant reduction (70%) in the migration coefficient, making it an optimal design for improving chloride penetration resistance.
4. Specific Electrical Resistance. Different mix designs exhibited varying specific electrical resistance values. SCC had the highest resistance, while the Z(0.2)+SF(7)+Na(2) design showed the lowest. Using xanthan gum as a standalone additive resulted in a remarkable 140% increase in the specific electrical resistance. Designs incorporating only micro-silica or nano-silica also demonstrated increased resistance compared to the control concrete. The design with 2% nano-silica, considered the optimal additive material, exhibited a 33% increase in the specific electrical resistance.

These findings provide valuable insights into the effects of different additives on the performance of concrete mix designs, particularly in terms of durability, chloride penetration resistance, and mechanical properties. They contribute to the existing body of knowledge and can inform the development of enhanced concrete mixes with improved characteristics.

The artificial neural network (ANN) analysis utilized four neurons in the hidden layer to mitigate the risk of overfitting, optimizing the model's performance while ensuring its generalization capabilities. The results of the ANN analysis showed good agreement with the chosen configuration, confirming the effectiveness of the selected neural network architecture. The findings of this study align with previous research in the field, including studies by Bušić et al. [46] on the durability performance and thermal resistance of self-compacting concrete improved with waste rubber and silica fume, Christopher Gnana raj [47] on the impact of additives on SCC and their effects on mechanical behavior, and Montag et al. [48] who presented a rapid chloride migration test to evaluate chloride penetration resistance under different conditions. The consistency between these studies reinforces the credibility and relevance of the current findings within the broader scientific context. Additionally, the studies referenced in [49–51] support the results obtained in this study.

8. Conclusions

To sum up, this study makes a significant contribution to the understanding of self-compacting concrete (SCC) by thoroughly investigating its rheological properties and the impact of various additives on critical parameters. The extensive examination of 43 mix designs, coupled with sensitivity analysis and expert opinions, provides a robust framework for optimizing concrete performance and prioritizing research additives. The utilization of a backpropagation neural network model for accurate prediction sets a new standard in evaluating the resistance and durability of SCC.

The findings of the study reveal novel insights into the behavior of SCC and the effectiveness of different additives. The significant reduction in penetration depth achieved by incorporating nano-silica, micro-silica, and xanthan gum demonstrates the potential for enhancing the durability of concrete structures. The double mix designs incorporating combinations of xanthan gum with micro-silica or nano-silica show promising advancements in resistance to chloride ion penetration, promoting more sustainable and long-lasting construction practices.

The observed improvements in compressive strength indicate the positive influence of additives on the mechanical properties of SCC. The decrease in the migration coefficient across all additive combinations highlights the enhanced resistance to chloride ion migration, which is essential for protecting concrete structures from deterioration in aggressive environments. Additionally, the specific electrical resistance results fur-

ther demonstrate the superior performance of SCC when incorporating xanthan gum, micro-silica, and nano-silica.

The inclusion of a proper component selection method for determining the optimal number of neurons in the hidden layer of the neural network model addresses the overfitting concerns and ensures the model's generalization capabilities. This innovative approach to predictive modeling showcases the potential of advanced computational techniques in optimizing concrete mix designs and improving construction practices.

By aligning with previous research and validating its findings, this study solidifies its position within the scientific community. The exceptional performance of the neural network model, the prioritization of research additives through sensitivity analysis, and the comprehensive investigation of SCC properties make this paper a significant and innovative contribution to the field of concrete technology. The findings have far-reaching implications for the design and implementation of durable and sustainable concrete structures, promoting a more resilient built environment.

Author Contributions: Conceptualization, A.M. and R.F.; methodology, A.M. and R.F.; software A.M.; validation, R.F. and S.H.G.; formal analysis, A.M. and R.F.; investigation, A.M., S.H.G. and R.F.; resources, A.M., S.H.G. and R.F.; data curation, A.M. and R.F.; writing—original draft preparation, A.M.; writing—review and editing, S.H.G.; visualization, A.M. and R.F.; supervision, S.H.G. and R.F.; project administration, R.F. and A.M.; funding acquisition, A.M. All authors have read and agreed to the published version of the manuscript.

Funding: This research received no external funding.

Data Availability Statement: The data presented in this study are available in the body of this paper.

Conflicts of Interest: The authors declare that they have no known competing financial interests or personal relationships that could have appeared to influence the work reported in this paper.

References

1. Pavithra, A.; Murali, K. Crushed-stone sand for use in the development of self-compacting concrete (SCC). *Mater. Today Proc.* **2023**, *in press*. [CrossRef]
2. Goodier, C.I. Development of self-compacting concrete. *Proc. ICE-Struct. Build.* **2003**, *156*, 405–414. [CrossRef]
3. Sonebi, M.; Rooney, M.; Bartos, P.J.M. Evaluation of the segregation resistance of fresh self-compacting concrete using different test methods. In Proceedings of the SCC, 1st International Symposium on Design, Performance and Use of Self-Consolidating Concrete, Xiamen, China, 5–8 June 2008; RILEM Publications: Changsha, China, 2008; pp. 301–308.
4. Sonebi, M.; Grünewald, S.; Walraven, J. Filling ability and passing ability of self-consolidating concrete. *ACI Mater. J.* **2007**, *104*, 162–170.
5. Sainz-Aja, J.; Thomas, C.; Polanco, J.A.; Carrascal, I. High-frequency fatigue testing of recycled aggregate concrete. *Appl. Sci.* **2019**, *10*, 10. [CrossRef]
6. Seelapureddy, J.J.; Bommisetty, J.; Seshagiri, R.M.V. Effect of metakaolin and micro silica on strength characteristics of standard grades of self-compacting concrete. *Mater. Today Proc.* **2021**, *45*, 884–890. [CrossRef]
7. Al-Hadithia, A.I.; Hilal, N.H. The possibility of enhancing some properties of self-compacting concrete by adding waste plastic fibers. *J. Build. Eng.* **2016**, *8*, 20–28. [CrossRef]
8. Al-Hadithia, A.I.; Ahmed, T.N.; Waseem, K.M. Mechanical properties and impact behavior of PET fiber reinforced self-compacting concrete (SCC). *Compos. Struct.* **2019**, *224*, 111021. [CrossRef]
9. Mahmoud, K.M.; Abdulkader, I.A.; Marwa, H.M. Production and optimization of ecoefficient self-compacting concrete SCC with limestone and PET. *Constr. Build.* **2019**, *197*, 734–746.
10. Faraj, R.H.; Mohammed, A.A.; Omer, K.M. Self-compacting concrete composites modified with nanoparticles: A comprehensive review, analysis and modeling. *J. Build. Eng.* **2022**, *50*, 104170. [CrossRef]
11. Vivek, S.S.; Dhinakaran, G. Effect of silica fume in flow properties and compressive strength of self compacting concrete. *Int. J. Chem. Tech. Res.* **2015**, *8*, 1–5.
12. Huang, F.; Li, H.; Yi, Z.; Wang, Z.; Xie, Y. The rheological properties of self-compacting concrete containing superplasticizer and air-entraining agent. *Constr. Build. Mater.* **2018**, *166*, 833–838. [CrossRef]
13. Liu, L.; Lei, M.; Gong, C.; Gan, S.; Yang, Z.; Kang, L.; Jia, C. A robust mix design method for self-compacting concrete. *Constr. Build. Mater.* **2022**, *352*, 128927. [CrossRef]
14. Nandhini, K.; Ponmalar, V. Microstructural behaviour and flowing ability of self-compacting concrete using micro- and nano-silica. *Micro Nano Lett.* **2018**, *13*, 1213–1218.

15. Neiwiadomski, P.; Stefaniuk, D.; Hola, J. Microstructural analysis of self-compacting concrete modified with the addition of nanoparticles. *Procedia Eng.* **2017**, *172*, 776–783. [CrossRef]
16. Dinesh, A.; Harini, S.; Jeba, P.J.; Jincy, J.; Shagufta, J. Experimental study on self compacting concrete. *Int. J. Eng. Sci. Res. Technol.* **2017**, *6*, 42–50.
17. Rao, S.V.; Rao, M.V.S.; Ramaseshu, D.P.; Rathish, K. Durability performance of self-compacting concrete. *Mag. Concr. Res.* **2015**, *64*, 1–5.
18. Vivek, S.S.; Dhinakaran, G. Fresh and hardened properties of binary blend high strength self compacting concrete. *Eng. Sci. Technol.-An. Int. J.* **2017**, *20*, 1173–1179. [CrossRef]
19. Hendi, A.; Rahmani, H.; Mostofinejad, D.; Tavakolinia, A.; Khosravi, M. Simultaneous effects of microsilica and nanosilica on selfconsolidating concrete in a sulfuric acid medium. *Constr. Build. Mater.* **2017**, *152*, 192–205. [CrossRef]
20. Nandhini, K.; Ponmalar, V. Investigation on nanosilica blended cementitious systems on the workability and durability performance of self-compacting concrete. *Mater. Express* **2020**, *10*, 10–20. [CrossRef]
21. Singh, B.; Singh, B. Influence of graphene-oxide nanosheets impregnation on properties of sterculia gum-polyacrylamide hydrogel formed by radiation induced polymerization. *Int. J. Biol. Macromol.* **2017**, *99*, 699–712. [CrossRef]
22. Sharma, K.; Kumar, V.; Kaith, B.S.; Kumar, V.; Som, S.; Kalia, S. Synthesis, characterization and water retention study of biodegradable Gum ghatti-poly (acrylic acid-aniline) hydrogels. *Polym. Degrad. Stab.* **2015**, *111*, 20–31. [CrossRef]
23. Kharkar, P.M.; Kiick, K.L.; Kloxin, A.M. Designing degradable hydrogels for orthogonal control of cell microenvironments. *Chem. Soc. Rev.* **2013**, *42*, 7335–7372. [CrossRef] [PubMed]
24. Popa, N.; Novac, O.; Profire, L.; Lupusoru, C.E.; Popa, M.I. Hydrogels based on chitosan-xanthan for controlled release of theophylline. *J. Mater. Sci. Mater. Med.* **2010**, *21*, 145–152. [CrossRef] [PubMed]
25. Alhalmi, A.; Ali, N.H.; Altowairi, M.; Almoiliqy, M.; Sharma, B. Xanthan gum; its biopharmaceutical applications: An overview. *World J. Pharm. Pharm. Sci.* **2018**, *7*, 1536–1548.
26. Garcia-Ochoa, F.; Mazorra, V.E.S.; Casas, J.A.; Jose, A.; Gomez, E. Xanthan gum: Production, recovery, and properties. *Biotechnol. Adv.* **2000**, *18*, 549–579. [CrossRef]
27. Harcum, W.W.; Barnum, P.E. Pharmaceutical applications of naturally occurring water-soluble polymers. *PSTT* **2015**, *1*, 254–261.
28. Rosalam, S.; England, R. Review of Xanthan gum production from unmodified starches by *Xanthomonas comprestris* sp. *Enzyme Microb. Technol.* **2006**, *39*, 197–207. [CrossRef]
29. Becker, A.; Katzen, F.; Puhler, A.; Ielpi, L. Xanthan gum biosynthesis and application: A biochemical/genetic perspective. *Appl. Microbiol.* **1998**, *50*, 145–152. [CrossRef]
30. Gils, P.S.; Ray, D.; Sahoo, P.K. Characteristics of xanthan gum-based biodegradable superporous hydrogel. *Int. J. Biol. Macromol.* **2009**, *45*, 364–371. [CrossRef]
31. Palaniraj, A.; Jayaraman, V. Production, recovery and applications of xanthan gum by *Xanthomonas campestris*. *J. Food Eng.* **2001**, *106*, 1–12. [CrossRef]
32. Farrokhzad, M.; Jamali, R. Investigation of the effect of xanthan gum additive on the mechanical properties and durability of concrete. *Concr. Res.* **2019**, *13*, 129–141.
33. Reinoso, D.; Martín-Alfonso, M.J.; Luckham, P.F.; Martínez-Boza, F.J. Rheological characterisation of xanthan gum in brine solutions at high temperature. *Carbohydr. Polym.* **2019**, *203*, 103–109. [CrossRef]
34. *ISIRI Number 389*; Specification for Portland Cement, 8th Edition. Institute of Standards and Industrial Research of Iran (ISIRI): Tehran, Iran, 2001.
35. *EN 197-1*; Cement: Composition, Specifications and Conformity Criteria, Part 1: Common Cements, EN/TC51/WG 6 rev. European Committee for Standardization: Bruxelles, Belgium, 2000.
36. *ASTM C1621/C1621M-17*; Standard Test Method for Passing Ability of Self-Consolidating Concrete by J-Ring. ASTM International: West Conshohocken, PA, USA, 2009.
37. Roussel, N. The LCPC BOX: A cheap and simple technique for yield stress measurements of SCC. *Mater. Struct.* **2007**, *40*, 889–896. [CrossRef]
38. EFNARC. *Specification and Guidelines for Self Compacting Concrete*; EFNARC: Surrey, UK, 2002.
39. *ASTM Standard C33*; Specification for Concrete Aggregates. ASTM International: West Conshohocken, PA, USA, 2003.
40. *AASHTO TP 64-03*; Standard Method of Test for Prediction of Chloride Penetration in Hydraulic Cement Concrete by the Rapid Migration Procedure. American Association of State Highway and Transportation Officials: Washington, DC, USA, 2003.
41. *NT BUILD 492*; Concrete, Mortar and Cement-Based Repair Materials: Concrete, Mortar and Cement-Based Repair Materials: Chloride Migration Coefficient from Non-Steady-State Migration Experiments. Nordtest: Espoo, Finland, 1999.
42. Malinowski, P.; Ziembicki, P. Analysis of district heating network monitoring by neural networks classification. *J. Civil. Eng. Manag.* **2006**, *12*, 21–28. [CrossRef]
43. Gao, H.; Wang, X.; Wu, K.; Zheng, Y.; Wang, Q.; Shi, W.; He, M. A review of building carbon emission accounting and prediction models. *Buildings* **2023**, *13*, 1617. [CrossRef]
44. Deng, Y.; Zhou, X.; Shen, J.; Xiao, G.; Hong, H.; Lin, H.; Wu, F.; Liao, B.Q. New methods based on back propagation (BP) and radial basis function (RBF) artificial neural networks (ANNs) for predicting the occurrence of haloketones in tap water. *Sci. Total Environ.* **2021**, *772*, 145534. [CrossRef] [PubMed]

45. Hao, C.-Y.; Shen, C.-H.; Jan, J.-C.; Hung, S.-K. A computer-aided approach to pozzolanic concrete mix design. *Adv. Civ. Eng.* **2018**, *2018*, 398017.
46. Bušić, R.; Miličević, I.; Dokšanović, T.; Grubišić, M. Durability performance and thermal resistance of structural self-compacting concrete improved with waste rubber and silica fume. *Buildings* **2023**, *13*, 1331. [CrossRef]
47. Gnanaraj, S. Effects of admixtures on the self compacting concrete state of the art report. *Conf. Ser Mater. Sci. Eng.* **2020**, *1006*, 012038. [CrossRef]
48. Montag, C.; Kannen, C.; Schivinski, B.; Pontes, H.M. Empirical evidence for robust personality-gaming disorder associations from a large-scale international investigation applying the APA and WHO frameworks. *PLoS ONE* **2021**, *16*, 0261380. [CrossRef]
49. Jiang, H.; Guoliang, L.; Alyami, G.H.; Abdullah, A.H.; Jameel, M.; Khadimallah, M.A. Intelligence decision mechanism for prediction of compressive strength of self-compaction green concrete via neural network. *J. Cleane Prod.* **2022**, *340*, 130580. [CrossRef]
50. Grabiec, A.M. Influence of viscosity modifying agent on some rheological properties, segregation resistance and compressive strength of self-compacting concrete. *J. Civil. Eng. Manag.* **2013**, *19*, 1–8. [CrossRef]
51. El Asri, Y.; Aicha, M.B.; Zaher, M.; Alaoui, A.H. Modelization of the rheological behavior of self-compacting concrete using artificial neural networks. *Mater. Today Proc.* **2022**, *58*, 1114–1121.

Disclaimer/Publisher's Note: The statements, opinions and data contained in all publications are solely those of the individual author(s) and contributor(s) and not of MDPI and/or the editor(s). MDPI and/or the editor(s) disclaim responsibility for any injury to people or property resulting from any ideas, methods, instructions or products referred to in the content.